

Characterization of viral insulins reveals white adipose tissue-specific effects in mice



Martina Chrudinová¹, François Moreau², Hye Lim Noh³, Terezie Páníková⁴, Lenka Žáková⁴, Randall H. Friedline³, Francisco A. Valenzuela⁵, Jason K. Kim^{3,6}, Jiří Jiráček⁴, C. Ronald Kahn², Emrah Altindis^{1,*}

ABSTRACT

Objective: Members of the insulin/insulin-like growth factor (IGF) superfamily are well conserved across the evolutionary tree. We recently showed that four viruses in the *Iridoviridae* family possess genes that encode proteins highly homologous to human insulin/IGF-1. Using chemically synthesized single-chain (sc), i.e., IGF-1-like, forms of the viral insulin/IGF-1-like peptides (VILPs), we previously showed that they can stimulate human receptors. Because these peptides possess potential cleavage sites to form double chain (dc), i.e., more insulin-like, VILPs, in this study, we have characterized dc forms of VILPs for Grouper iridovirus (GIV), Singapore grouper iridovirus (SGIV) and Lymphocystis disease virus-1 (LCDV-1) for the first time.

Methods: The dcVILPs were chemically synthesized. Using murine fibroblast cell lines overexpressing insulin receptor (IR-A or IR-B) or IGF1R, we first determined the binding affinity of dcVILPs to the receptors and characterized post-receptor signaling. Further, we used C57BL/6J mice to study the effect of dcVILPs on lowering blood glucose. We designed a 3-h dcVILP in vivo infusion experiment to determine the glucose uptake in different tissues.

Results: GIV and SGIV dcVILPs bind to both isoforms of human insulin receptor (IR-A and IR-B) and to the IGF1R, and for the latter, show higher affinity than human insulin. These dcVILPs stimulate IR and IGF1R phosphorylation and post-receptor signaling in vitro and in vivo. Both GIV and SGIV dcVILPs stimulate glucose uptake in mice. In vivo infusion experiments revealed that while insulin (0.015 nmol/kg/min) and GIV dcVILP (0.75 nmol/kg/min) stimulated a comparable glucose uptake in heart and skeletal muscle and brown adipose tissue, GIV dcVILP stimulated 2-fold higher glucose uptake in white adipose tissue (WAT) compared to insulin. This was associated with increased Akt phosphorylation and glucose transporter type 4 (GLUT4) gene expression compared to insulin in WAT.

Conclusions: Our results show that GIV and SGIV dcVILPs are active members of the insulin superfamily with unique characteristics. Elucidating the mechanism of tissue specificity for GIV dcVILP will help us to better understand insulin action, design new analogs that specifically target the tissues and provide new insights into their potential role in disease.

© 2020 The Authors. Published by Elsevier GmbH. This is an open access article under the CC BY-NC-ND license (<http://creativecommons.org/licenses/by-nc-nd/4.0/>).

Keywords VILPs; Viral insulin; Insulin; IGF-1; GLUT4; Adipose tissue; Glucose metabolism; Viral mimicry

1. INTRODUCTION

In vertebrates, the insulin gene superfamily includes insulin, two insulin-like growth factors (IGF-1 and IGF-2), and more distant hormones, including relaxin and the Leydig insulin-like peptides [1]. Insulin-like peptides have also been identified in invertebrates, including insects, mollusks, and nematodes [2–5]. These ligands are well conserved across the phylogenetic tree. However, their functions vary from the control of longevity and stress resistance in invertebrates to the control of metabolism and cell growth in vertebrates [5]. In

mammals, insulin mainly regulates glucose and lipid metabolism [6], whereas IGF-1 and IGF-2 predominantly control cell growth, proliferation, and differentiation [7]. Insulin and IGF-1 bind to two different tyrosine kinase receptors in mammals: the insulin receptor, which itself exists in two isoforms (IR-A and IR-B), and the IGF-1 receptor (IGF1R) [7]. Invertebrates, on the other hand, often have multiple insulin-like peptides and elicit their biological function through one receptor or, in rare cases, through multiple receptors [2–4,8]. A major difference between insulin and IGF-1/2 is their ability to be processed post-transcriptionally into either a two-chain peptide hormone, in the

¹Boston College Biology Department, Higgins Hall, 140 Commonwealth Avenue Chestnut Hill, MA, 02467, USA ²Section of Integrative Physiology and Metabolism, Joslin Diabetes Center, Harvard Medical School, Boston, MA, 02215, USA ³Program in Molecular Medicine, Department of Medicine, University of Massachusetts Medical School, Worcester, MA, 01655, USA ⁴Institute of Organic Chemistry and Biochemistry, Czech Academy of Sciences, Flemingovo n. 2, 166 10 Prague 6, Czech Republic ⁵Eli Lilly and Company, Indianapolis, IN, USA ⁶Division of Endocrinology, Metabolism and Diabetes, Department of Medicine, University of Massachusetts Medical School, Worcester, MA, 01655, USA

*Corresponding author. E-mail: altindis@bc.edu (E. Altindis).

Abbreviations: VILP, viral insulin/IGF-like peptide; sc, single chain; dc, double chain; GIV, Grouper iridovirus; SGIV, Singapore grouper iridovirus; LCDV-1, Lymphocystis disease virus 1

Received August 28, 2020 • Revision received November 5, 2020 • Accepted November 16, 2020 • Available online 19 November 2020

<https://doi.org/10.1016/j.molmet.2020.101121>

case of insulin, or a single-chain peptide hormone, in the case of IGF-1/2.

We recently showed that four viruses that belong to *Iridoviridae* family possess genes that show significant homology to human insulin/IGF-1 which we termed viral insulin/IGF-1-like peptides (VILPs) [9,10]. Although viruses encoding these sequences were originally isolated from fish [11–14], reanalyzing published human microbiome data, we identified the DNA of some of these viruses in human fecal and blood samples [9]. In our previous study, three VILPs were also chemically synthesized as single-chain peptides (sc), i.e., IGF-1-like peptides, and we showed that scVILPs are weak ligands of the insulin receptor but strong ligands of the IGF-1 receptor *in vitro* and also possessed some glucose lowering effects *in vivo* [9].

In humans, insulin is initially translated as an sc peptide (preproinsulin) in pancreatic β -cells containing a signal peptide (SP) followed by B-, C-, and A-domains (Figure 1, Fig. S1A). Proinsulin is formed in the endoplasmic reticulum by cleavage of the SP, and the C-peptide is removed in the secretory granules to form mature insulin, with A- and B- chains bound together by disulfide bonds [15]. Unlike insulin, IGF-1 is produced in multiple tissues, but primarily in the liver [16], and after cleavage of the signal peptide remains as a sc peptide consisting of A- and B-domains, a short C-domain, and an additional D-domain at the C-terminus (Figure 1A, Fig. S1B). The two peptide hormones show significant structural homology with approximately 50% of their amino acids being identical. Six cysteines that are crucial for the correct protein folding are also evolutionally conserved (Fig. S1). These cysteines are conserved throughout the phylogenetic tree [5,17,18] and are considered to be characteristic of the peptides belonging to the insulin/IGF peptide family. The main secondary structure motifs are also conserved between insulin and IGF-1, including the central α -helix in the B-chain/domain and two antiparallel α -helices in the A-chain/domain [19,20].

In this study, we have synthesized and characterized the dc (insulin-like) forms of three VILPs, Grouper Iridovirus (GIV), Singapore Grouper Iridovirus (SGIV), and Lymphocystis disease virus-1 (LCDV-1) VILPs, for the first time. Using *in vitro* assays, we show that both GIV and SGIV dcVILPs can bind to both isoforms of the human insulin receptor and human IGF1R and stimulate post-receptor signaling, while LCDV-1 dcVILP is a very weak ligand. GIV and SGIV dcVILPs can also stimulate glucose uptake *in vivo*. During *in vivo* infusion experiments in awake mice, GIV dcVILP preferentially stimulates glucose uptake in white adipose tissue (WAT) compared to other insulin-sensitive tissues. This is associated with higher Akt phosphorylation and expression of GLUT4 gene upon GIV dcVILP stimulation in WAT compared to insulin. Taken together, our results show that GIV and SGIV dcVILPs are potent members of the insulin/IGF family, and GIV dcVILP has unique WAT-specific characteristics.

2. MATERIALS AND METHODS

2.1. Bioinformatics

The sequence alignments presented in this paper were prepared using a multiple sequence alignment program (Clustal Omega). We used the website <https://swissmodel.expasy.org/> for the homologous building [21] and to align the modelled dcVILPs with insulin or IGF-1 in IR (PDB: 6PXV) or IGF1R structures (PDB: 6PYH). The final figures were prepared using PyMOL.

2.2. Peptide synthesis

Viral insulin-like peptides were synthesized via Fmoc solid phase peptide synthesis (SPPS) utilizing a commercial automated peptide

synthesizer (Symphony® X, Gyros Protein Technologies) using a similar method to what has been previously reported [22]. Briefly, A- and B-chains were individually synthesized at a 0.1 mmol scale using standard Fmoc-protected amino acids, a specific set of orthogonally side-chain protected cysteine residues that allows for directed disulfide bridge formation, pseudoproline and isoacyl dipeptide building blocks that aid in overcoming coupling difficulties during SPPS and ameliorate solubility issues during high-performance liquid chromatography (HPLC) purification, respectively. Fmoc deprotection was carried out using 20% piperidine in DMF, and coupling reactions were done using DIC/Oxyma for 1 h using a 9-fold excess of reagents. Fmoc-Rink-MBHA resin was used as the solid support for the synthesis of the A-chains. The cysteine protection arrangement used for GIV and SGIV dcVILPs A-chains was as follows: Cys (StBu)A6, Cys (Acm)A7, Cys (Mmt)A11, and Cys (Trt)A20. The Cysteine protection arrangement used for LCDV-1 dcVILP A-chain was as follows: Cys (STmp)A6, Cys (Acm)A7, Cys (Mmt)A12, and Cys (Trt)A21. While no isoacyl dipeptides were used for GIV and SGIV dcVILPs A-chains, the LCDV-1 dcVILP A-chain required the use of Boc-Thr (Fmoc-Ala)-OH isoacyl dipeptide at positions A3,4 and Fmoc-Thr (tBu)-Thr ($^{15}\text{Me,MePro}$)-OH pseudoproline dipeptide at positions A8,9 and A13,14. A-chains are synthesized bearing the intramolecular disulfide bridge (CysA6-CysA11 for GIV and SGIV dcVILPs and CysA6-CysA12 for LCDV-1). This bond was formed during the SPPS process as outlined in Scheme 2 as reported by Liu et al. [22]. A slight deviation from Scheme 2 was necessary for the synthesis of LCDV-1 dcVILP A-chain in that Cys (STmp)A6 was deprotected with 0.1 M N-methylmorpholine and 5% dithiothreitol in DMF instead of 25% β -mercaptoethanol in DMF. B-chains for GIV and SGIV dcVILPs were synthesized on Fmoc-Arg (Pbf)-Wang resin, and the B-chain for LCDV-1 dcVILP was carried out using H-Thr (tBu)-HMPB-ChemMatrix resin. The cysteine protection arrangement used for GIV, SGIV, and LCDV-1 dcVILPs B-chains was as follows: Cys (Acm)B7, and Cys (Trt)B19. While no isoacyl dipeptide was used for the LCDV-1 dcVILP B-chain, GIV, and SGIV dcVILPs B-chains included the use of Boc-Thr [Fmoc-Tyr (tBu)]-OH isoacyl dipeptide at positions B25,26. The final solid support cleavage and global side chain deprotection was achieved using standard trifluoroacetic acid (TFA)-mediated acidolysis protocols, with the inclusion of DTNP in the cleavage cocktail of the B-chains to yield the activated Cys (SNpy)19 residue. The A- and B-chains were purified using standard reverse phase HPLC methods (TFA acidified water/acetonitrile mobile phases) and were lyophilized to dryness after purification. The intermolecular disulfide bridges CysA20-CysB19, ACys7-CysB7 for GIV and SGIV dcVILPs; and CysA21-CysB19, CysA7-CysB7 for LCDV-1 dcVILPs were formed in a guided and sequential manner exploiting the orthogonality of the cysteine protection scheme. A-chains, B-chains, intermediates, and the final dcVILPs were characterized by analytical liquid chromatography mass spectrometry (LC-MS), purified by RP-HPLC, and lyophilized to dryness.

2.3. Cell culture

Human IM-9 lymphocytes (ATCC) and murine embryonic fibroblasts, which were derived from IGF1R knockout mice and stably transfected with either IR-A (R⁻/IR-A cells), IR-B (R⁻/IR-B cells), or IGF1R (R⁺³⁹ cells), kindly provided by A. Belfiore (Catanzaro, Italy) and R. Baserga (Philadelphia, PA), were cultured as described previously [23,24].

2.4. Receptor binding studies

For receptor binding studies, human IM-9 lymphoblasts, that express IR-A exclusively, and R⁻/IR-B and R⁺³⁹ murine embryonic fibroblasts (described above) were used for a whole-cell receptor-binding assay.

Receptor binding assays with IR-A were performed according to Morcavallo et al. [24], and binding assays with IR-B and IGF1R were performed according to Kosinova et al. [25]. The binding curve of each ligand was determined in duplicate, and the final dissociation constant (K_d) was calculated from at least three ($n \leq 3$) binding curves. Human insulin and human IGF-1 were supplied by Merck. Human ^{125}I -insulin (NEX420050UC) and human ^{125}I -IGF-1 (NEX241025UC) were supplied by Perkin–Elmer.

2.5. Receptor phosphorylation and downstream signaling

For receptor phosphorylation and downstream signaling experiments, $R^-/IR-A$, $R^-/IR-B$, and R^{+39} murine embryonic fibroblasts (described above) were used to explore signaling properties of ligands via specific receptors. Cells were seeded into 24-well plates (Denville Scientific) (8×10^4 cells per well) in 300 μl of Dulbecco's modified Eagle's medium (DMEM, Corning) supplemented with 10% fetal bovine serum (FBS, Corning) and grown overnight. Afterward, cells were washed twice with phosphate-buffered saline (PBS) and starved in serum-free media for 4 h. After the starvation, cells were washed with pure DMEM media and incubated with ligand diluted in pure DMEM media (0, 1, 10, 100, and 250 nM) in 37 °C for 5 or 15 min. The reaction was terminated by washing the cells with ice-cold PBS (HyClone) followed by snap freezing in liquid nitrogen. Cell lysis was performed using 50 μl of radioimmunoprecipitation assay (RIPA) buffer (Millipore) supplemented with protease and phosphatase inhibitors (Bimake). Cells on plates were incubated in the RIPA buffer on ice for 15 min, then transferred to microtubes and incubated on ice for additional 15 min. The lysates were centrifuged (13,000 g, 5 min, 4 °C) and supernatant was transferred to new microtubes. Protein concentration in each sample was evaluated using BCA Assay (Thermo Fisher Scientific). Samples were further diluted using sample buffer for sodium dodecyl sulfate polyacrylamide gel electrophoresis (SDS-PAGE, final concentration 62.5 mM Tris, 2% SDS (w/v), 10% glycerol (v/v), 0.01% bromophenol blue (w/v), 0.1M DTT (w/v), pH = 6.8 (HCl)) and routinely analyzed using SDS-PAGE and immunoblotting. Cell lysates (4 μg of protein content/sample) were separated on 10% polyacrylamide gels and electroblotted to PVDF membrane. The membranes were probed with primary antibodies against phospho-IR/IGF1R (1:500, #3024), phospho-Akt (S473) (1:1,000, #9271) and phospho-Erk1/2 (T202/Y204) (1:5,000, #9101). All primary antibodies against phosphoproteins were purchased from Cell Signaling Technology. The western blots were developed using SuperSignal West Pico PLUS Sensitivity substrate (Thermo Fisher Scientific). For detection of the amount of total proteins, standard stripping procedure using the mild stripping buffer (1.5% glycine (w/v), 0.1% SDS (w/v), 1% Tween20 (v/v), pH = 2.2 (HCl)) was used, and the membranes were relabeled with primary antibodies against IR β (1:1,000, #3025), IGF1R β (1:1,000, #9750), Akt (1:1,000, #4685), and Erk1/2 (1:2,000, #9102). All primary antibodies against total proteins were purchased from Cell Signaling Technology. HRP Goat Anti-Rabbit secondary antibody was used in all cases (1: 10,000, ABclonal #AS014).

To exclude the possibility that VILPs could stimulate insulin/IGF signaling via other membrane receptors, we performed a signaling experiment on double-knockout (DKO) murine preadipocytes that lack both IR and IGF1R [26]. In this experiment, the cells were stimulated with high concentration (500 nM) of each ligand for 15 min at 37 °C.

2.6. Insulin tolerance test

All animal studies presented in this study complied with the regulations and ethics guidelines of the National Institutes of Health (NIH)

and were approved by the Boston College Institutional Animal Care and Use Committee. Insulin tolerance testing was performed on 12- to 20-week-old male C57BL/6J mice (Jackson Laboratory). Mice were grouped according to their weight before experiment. After a 4-hour starvation, mice were injected intraperitoneally (i.p.) with insulin (Humulin, 6 nmol/kg (corresponds to 1.0 U/kg) (Eli Lilly)), GIV and SGIV dcVILPs (0.3 $\mu\text{mol/kg}$ or 60 nmol/kg), LCDV-1 dcVILP (1 $\mu\text{mol/kg}$), and saline as a control ($n = 5$ per condition). Tail-vein blood glucose was measured at the indicated time points (Figure 3) using an Infinity glucometer (US Diagnostic, Inc.). Statistical analysis was performed using mixed effects analysis and Dunnett's multiple comparisons test.

2.7. In vivo infusion experiments in awake mice

All in vivo infusion experiments in mice were conducted at the National Mouse Metabolic Phenotyping Center (MMPC) at UMass Medical School, and animal studies were approved by the Institutional Animal Care and Use Committee of the University of Massachusetts Medical School. Male C57BL/6J mice received a survival surgery to establish an indwelling catheter in the right internal jugular vein. After recovery of 4–5 days, mice were fasted overnight (16 h) and placed in rat-sized restrainers for in vivo experiments. In the dose optimization experiment, mice received a continuous infusion of insulin (0.015 nmol/kg/min, corresponds to 2.5 mU/kg/min, $n = 4$) or GIV (0.15 nmol/kg/min or 1.5 nmol/kg/min, $n = 2$ for each group) for 2 h, and 20% glucose was infused at variable rates to maintain euglycemia. Blood samples were collected from the tail tip at 10-min intervals to measure plasma glucose levels during the 2-hour experiments. The experiment was later repeated using continuous infusion of the same concentration of insulin (0.015 nmol/kg/min, $n = 4$), GIV dcVILP (0.75 nmol/kg min, $n = 4$), or saline ($n = 4$).

Additional cohort of male C57BL/6J mice received a continuous infusion of insulin (0.015 nmol/kg/min, $n = 5$), GIV dcVILP (0.75 nmol/kg/min, $n = 5$) or saline ($n = 6$) for 3 h, and 20% glucose was infused at variable rates to maintain euglycemia. During the experiments, [$3\text{-}^3\text{H}$]glucose (PerkinElmer, Waltham, MA) was continuously infused for 3 h to assess whole body glucose turnover, and 2-deoxy-D-[1- ^{14}C]glucose was administered as a bolus (10 μCi) 45 min before the end of experiments to measure glucose uptake in individual organs [27]. Blood samples were collected from the tail tip at 10- to 20-minute intervals during the experiments. At the end of experiments, mice were euthanized, and tissues (skeletal muscle, liver, BAT, WAT, and heart) were harvested, snap frozen in liquid nitrogen, and kept at -80 °C for biochemical analysis. Statistical analysis was done using two-way repeated measures analysis of variance (ANOVA) followed by Tukey's multiple comparisons test.

2.8. Biochemical analysis of glucose metabolism

Glucose concentrations were analyzed using 5 μl of plasma by a glucose oxidase method on Analox GM9 Analyzer (Analox Instruments Ltd., Hammersmith, London, UK). Plasma concentrations of [$3\text{-}^3\text{H}$]glucose and 2-deoxy-D-[1- ^{14}C]glucose were determined following deproteinization of plasma samples as previously described [27]. For the determination of tissue 2-[^{14}C]DG-6-phosphate (2-[^{14}C]DG-6-P) content, tissue samples were homogenized, and the supernatants were subjected to an ion exchange column to separate 2-[^{14}C]DG-6-P from 2-[^{14}C]DG. Glucose uptake in individual tissues was assessed by determining the tissue content of 2-[^{14}C]DG-6-P and plasma 2-[^{14}C]DG profile.

2.9. Molecular analysis using tissues collected from in vivo infusion experiments

The following molecular analysis (insulin signaling, RNA isolation, and reverse transcription quantitative polymerase chain reaction (RT-qPCR) was performed using tissue samples collected from in vivo infusion experiments at the National MMPC at UMass Medical School. Male C57BL/6J mice received a continuous infusion of insulin (0.015 nmol/kg/min) or GIV dcVILP (0.75 nmol/kg/min), or saline (n = 4–6) for 3 h, and 20% glucose was infused at variable rates to maintain euglycemia. Blood samples were collected from the tail tip at 10- to 20-minute intervals during the experiments. Basal tissue samples were collected after a 3-hour infusion of saline in awake mice.

2.10. In vivo insulin signaling and GLUT4 determination

Tissues were lysed in RIPA buffer (EMD Millipore) supplemented with 0.1% SDS and a cocktail of protease and phosphatase inhibitors (BioTools). Proteins were denatured in denaturing buffer (NuPAGE LDS Sample Buffer, Thermo Fisher Scientific) supplemented with 5% β -mercaptoethanol and incubated at 90 °C for 5 min. Ten micrograms/well of protein was loaded on a 4–12% NuPAGE Bis-tris gel (Thermo Fisher Scientific) and then transferred to a polyvinylidene difluoride (PVDF) membrane (Thermo Fisher Scientific). The membrane was blocked in blocking buffer (Thermo Fisher Scientific) for 1 h at room temperature and incubated with primary antibody (1:1,000) overnight and with secondary antibody (1:1,000) for 4 h. The membranes were probed with the following antibodies: IR β (#3025S), phospho-IR/IGF1R (#3024L), Akt (#4685), and phospho-Akt (S473) (#4060) from Cell Signaling Technology, GLUT4 (#Ab654) from Abcam, and goat anti-rabbit HRP conjugate (#1706515) from Bio-Rad. Protein detection was performed using a combination of a luminol solution and a peroxide solution (1:1) (Thermo Fisher Scientific). Protein bands were detected with a ChemiDoc MP Imaging System (Bio-Rad) and quantified with ImageJ.

2.11. RNA isolation

Tissues were homogenized in 1 ml of QIAzol Lysis Reagent (Qiagen) using 0.1 mm dia Zirconia/Silica beads (Biospec) and Minibeadbeater (Biospec). After homogenization, samples were incubated for 5 min at room temperature (RT), centrifuged (12,000 g, 10 min, 4 °C), and supernatant was transferred to a new tube. In the case of BAT and WAT, an additional centrifugation step was included, and the upper fatty layer was avoided when transferred to new tubes. Two hundred microliters of chloroform (Sigma–Aldrich) was added, and the samples were vortexed for 15 s, incubated for 5 min at RT, and centrifuged (12,000g, 15 min, 4 °C). The aqueous phase was transferred to new tubes, 100% ethanol in ratio 1:1 was added, and subsequently, the Direct-zol RNA Miniprep Kit (Zymo Research) was used according to the manufacturer's instructions.

2.12. RT-qPCR

DNase treatment and cDNA synthesis was performed using the SuperScript™ IV VIL0™ Master Mix with ezDNase (Invitrogen) according to manufacturer's instructions. The qPCR was performed using Power SYBR® Green PCR Master Mix (Applied Biosystems) according to manufacturer's instructions on QuantStudio 3 (Applied Biosystems). The primers used are listed in Table S2.

3. RESULTS

3.1. dcVILPs show significant homology in primary and predicted 3D structures with human insulin and IGF-1

Comparative alignment analysis revealed that GIV, SGIV, and LCDV-1 dcVILPs show significant homology with human insulin and IGF-1

(Table 1, Fig. S1). All VILPs carry the six cysteine residues that form intrachain and interchain disulfide bonds and are critical for correct folding of insulin/IGF-like molecules (Fig. S1). While GIV and SGIV dcVILPs only differ in three amino acids within their A- and B-chains, the similarity between LCDV-1 and GIV/SGIV dcVILPs is lower, with LCDV-1 sharing only 40% of amino acids of the A- and B-chains with GIV and SGIV dcVILPs (Fig. S1). A significant number of the residues that have been previously shown to be involved in insulin:IR or IGF-1:IGF1R interaction [28–33] are either conserved or conservatively substituted in dcVILPs (Figure 1A, Table 1). Structural studies have suggested that the mature IR or IGF1R can bind two insulin or IGF-1 molecules with high affinity, effectively crosslinking two binding sub-sites on IR/IGF1R named as Site 1 and Site 2 [28–30,34–36]. However, two recent studies have suggested that up to four insulin molecules can bind to IR [31,32] via two distinct binding sites. They named the new binding site “Site 2” and the previously identified sites “Site 1” [31,32]. In this manuscript, we used this new Site 1 and Site 2 nomenclature for IR binding. Interestingly, no analogic binding site to the new IR site 2 was identified in IGF1R [33]. To explore the similarity of 3D structures of dcVILPs with insulin, IGF-1, and its potential effect on binding to IR and IGF1R, we created models of dcVILPs bound to these receptors. These models indicate that residues conserved among dcVILPs, insulin, and IGF-1 take similar positions upon receptor binding. Insulin and IGF-1 bound to Site 1 of IR/IGF1R, respectively, and the predicted structures of GIV and LCDV-1 dcVILPs bound to Site 1 of the receptors are shown in Figure 1B–E.

3.2. GIV and SGIV dcVILPs bind to the human insulin and IGF-1 receptors

To determine the relative affinity of dcVILPs for the two isoforms of human insulin receptor (IR-A and IR-B) and the IGF-1 receptor, we tested their ability to compete with ¹²⁵I-insulin and ¹²⁵I-IGF-1 in a binding competition assay [24,25]. We used IM-9 lymphoblasts for IR-A binding competition since these cells exclusively express IR-A on their surface [37,38]. Murine embryonic fibroblasts cells derived from IGF1R knock-out mice [39] stably transfected with either human IR-B or human IGF1R were used to assess binding competition for IR-B and IGF1R [40,41]. Consistent with previous studies [42], we found that human IGF-1 binds to IR-A and IR-B with 200x and 300x lower affinity than human insulin, respectively. GIV dcVILP competes for binding to IR-A with an affinity 3x lower than human IGF-1, while the affinity of SGIV dcVILP was comparable to IGF-1. The relative affinity of the GIV and SGIV dcVILPs for IR-B was slightly lower, with levels 7–8x lower for both dcVILPs compared to IGF-1. Although LCDV-1 dcVILP has more identical residues to insulin than GIV and SGIV dcVILPs, we did not

Table 1 — Comparison of conserved residues among human insulin, human IGF-1, and dcVILPs. Percentage of amino acid residues that GIV, SGIV and LCDV-1 dcVILPs share with human insulin and IGF-1 is shown in upper panel. Percentage of amino acids that are important for receptor binding in dcVILPs is shown in the lower panel.

	A-chain/domain			B-chain/domain			
	dc GIV	dc SGIV	dc LCDV-1	dc GIV	dc SGIV	dc LCDV-1	
Insulin	38%	38%	52%	Insulin	30%	33%	47%
IGF-1	38%	38%	43%	IGF-1	45%	45%	59%
	Site 1 binding residues			Site 2 binding residues			
	dc GIV	dc SGIV	dc LCDV-1	dc GIV	dc SGIV	dc LCDV-1	
IR	71%	71%	59%	IR	43%	43%	64%
IGF1R	52%	52%	48%	IGF1R	—	—	—

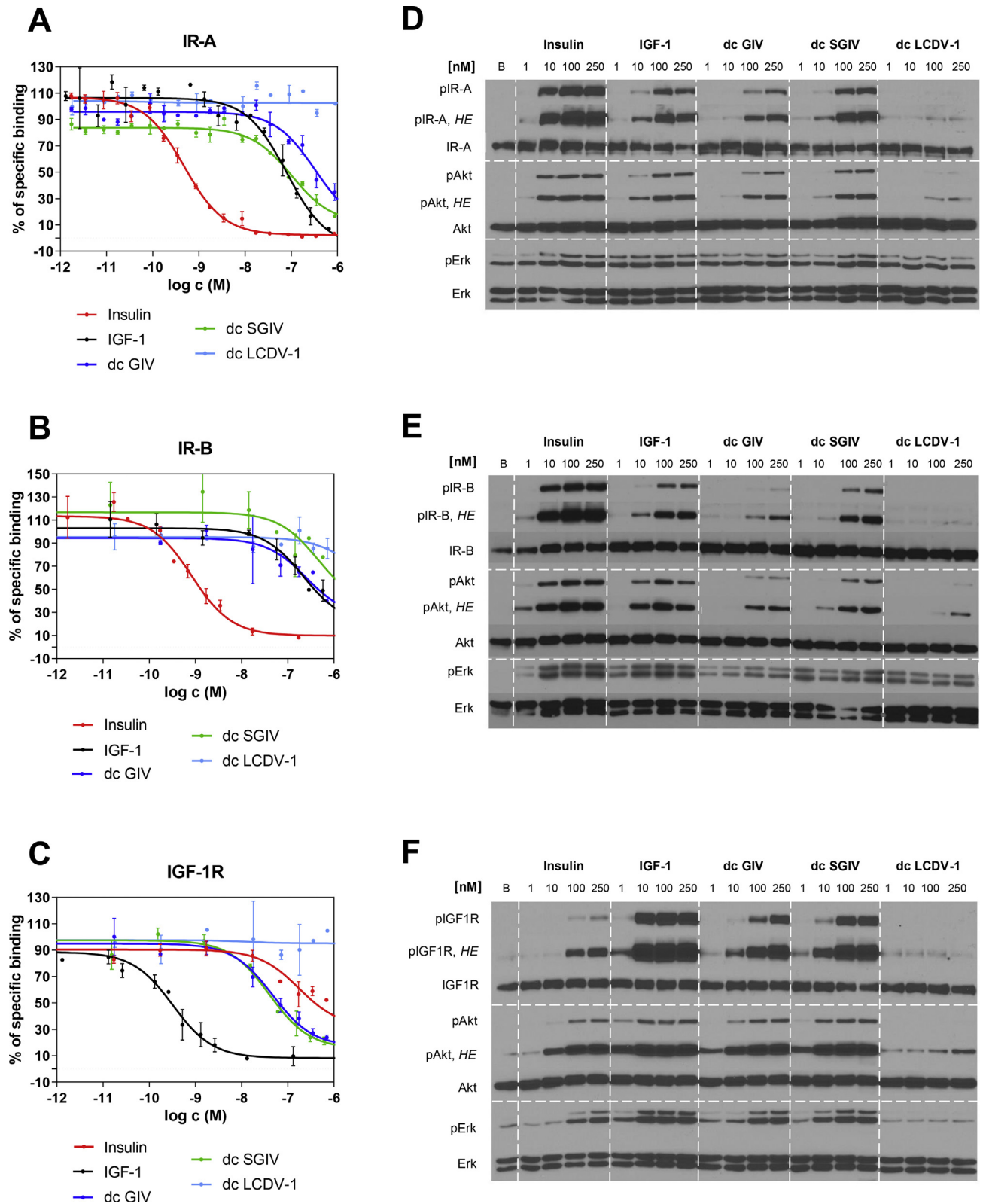


Figure 2: dcVILPs bind to human IR-A, IR-B, and IGF1R and stimulate insulin signaling. **A - C:** Binding competition dose response curves. The curves are showing the ability of dcVILPs to compete with ¹²⁵I-labeled human insulin for binding to IR-A (**A**) and IR-B (**B**) and with ¹²⁵I-labeled human IGF-1 for binding to IGF1R (**C**). IM-9 cells were used for measurements on IR-A, while murine embryonic fibroblasts derived from IGF-1 knock-out mice and stably transfected with either human IR-B or human IGF1R were used for measurements on these receptors. A representative curve for each peptide to each receptor is shown. Each point represents the mean ± SEM of duplicates. Every experiment was repeated at least three times. **D - F:** Insulin signaling via IR-A (**D**), IR-B (**E**), and IGF1R (**F**). Murine embryonic fibroblasts derived from IGF-1 knock-out mice and stably transfected with either human IR-A, IR-B or human IGF1R were used for the experiment. Phosphorylation of the specific receptor, Akt and Erk1/2 was observed in 15 min after stimulation. Exposure times were between 30 s and 1 min. High exposure time (HE) was 5 min.

observe any binding competition with this ligand (Figure 2A,B, Table 2). The affinity of insulin for IGF1R was 1000x lower compared to IGF-1, consistent with previous studies [42]. Thus, even as double-chain peptides, GIV and SGIV dcVILPs had higher affinity for IGF1R than insulin by 7- to 10-fold. We did not observe any binding competition for LCDV-1 dcVILP for IGF1R (Figure 2C, Table 2).

3.3. dcVILPs stimulate downstream insulin/IGF signaling via human IR-A, IR-B, and IGF1R

To explore the effects of the dcVILPs on post-receptor signaling, we used the murine embryonic fibroblasts defined above that overexpress either human IR-A, IR-B, or IGF1R [40,41]. Insulin/IGF-1 acting through their respective receptors activate (i) the PI3K/Akt pathway, that mainly regulates metabolic effects, and (ii) the Ras/MAPK pathway, that is responsible for mitogenic effects [43,44]. We tested receptor phosphorylation and phosphorylation of Akt for PI3K/Akt pathway activation and Erk1/2 for Ras/MAPK pathway activation.

On both IR isoforms, insulin induced the strongest dose—response for stimulation of the receptor autophosphorylation as expected. IGF-1 was less potent, such that stimulation with 250 nM of ligand was weaker than insulin at 10 nM (Figure 2D,E). GIV and SGIV dcVILPs stimulated insulin/IGF signaling in a dose-dependent manner. On IR-A, SGIV dcVILP stimulated receptor phosphorylation comparable to IGF-1, and GIV dcVILP was slightly less potent at all concentrations tested (Figure 2D). On IR-B, both peptides were slightly less potent compared to IGF-1 and comparable to each other (Figure 2E). Both GIV and SGIV dcVILPs stimulated phosphorylation of Akt and Erk1/2 in proportion to their effects on the receptor, with greater effects on IR-A than IR-B (Figure 2D,E). Interestingly, we observed a stronger Erk phosphorylation when comparing 1 nM dcVILPs with 1 nM human insulin. To determine whether this is related to the kinetics of the VILPs, we tested insulin/IGF signaling at an earlier time point (5-minute stimulation). At this time point, 1 nM of insulin stimulated a stronger Erk phosphorylation compared to 1 nM dcVILPs (Figs. S2A and B), suggesting potential delayed kinetics of dc VILPs. Although we did not observe any competition for binding with LCDV-1 dcVILP, we observed a weak Akt phosphorylation and receptor autophosphorylation on both IR-A and IR-B (Figure 2F).

Consistent with the binding competition results on IGF1R, SGIV and GIV dcVILPs stimulated post-receptor signaling more potent than insulin, with SGIV dcVILP being slightly more potent than GIV dcVILP. As observed for the IR, although we did not observe any binding competition for LCDV-1 dcVILP, it stimulated a weak signal for receptor

and Akt phosphorylation (Figure 2F). The results of insulin/IGF signaling assessed 5 min after stimulation were consistent with results obtained in 15 min (Fig. S2C).

In the murine preadipocytes that were knocked out for both IR and IGF1R [26], we did not observe any Akt or Erk phosphorylation, confirming that VILP action is directly mediated by IR and/or IGF1R (Fig. S3).

3.4. GIV and SGIV dcVILPs are active in vivo and stimulate glucose uptake in mice

To test whether dcVILPs can stimulate glucose uptake in vivo, we performed an insulin tolerance test (ITT). Adult C57BL/6J mice were injected intraperitoneally with either 6 nmol/kg of insulin or different concentrations of GIV and SGIV dcVILPs (Figure 3). Based on our in vitro data showing approximately 0.05% relative affinity for the IR, we decided to use 0.3 $\mu\text{mol/kg}$ (50x higher concentration than insulin) of GIV and SGIV dcVILPs in male mice. Consistent with previous studies [9,45], insulin caused a 60% decrease in blood glucose in 60 min, after which glucose started to increase. Surprisingly, injection with 50x GIV or SGIV dcVILPs led to very severe hypoglycemia, which required termination of the experiment in 30 min by injecting glucose to save the animals (Figure 3A).

When this experiment was repeated using 60 nmol/kg concentrations of the dcVILPs (10x) (Figure 3B,D), again, both dcVILPs were able to significantly lower the blood glucose, and at 60 min produced 57–58% of the effect of insulin (Figure 3B). By comparison, injection of IGF-1 at a concentration of 60 nmol/kg (10x) reached 71% of the effect of insulin at 60 min (Figure 3C). Similar results were obtained in female mice. Consistent with previous studies [46], female mice were more insulin-, IGF-1-, and VILP-sensitive compared to their male counterparts (Figure 3). Areas under the curve from these experiments are shown in supplementary material in Fig. S4. Taken together, these results indicate that both dcVILPs have in vivo glucose-lowering effects similar to IGF-1 but slightly more than an order of magnitude less potent than insulin and with a longer duration of effect.

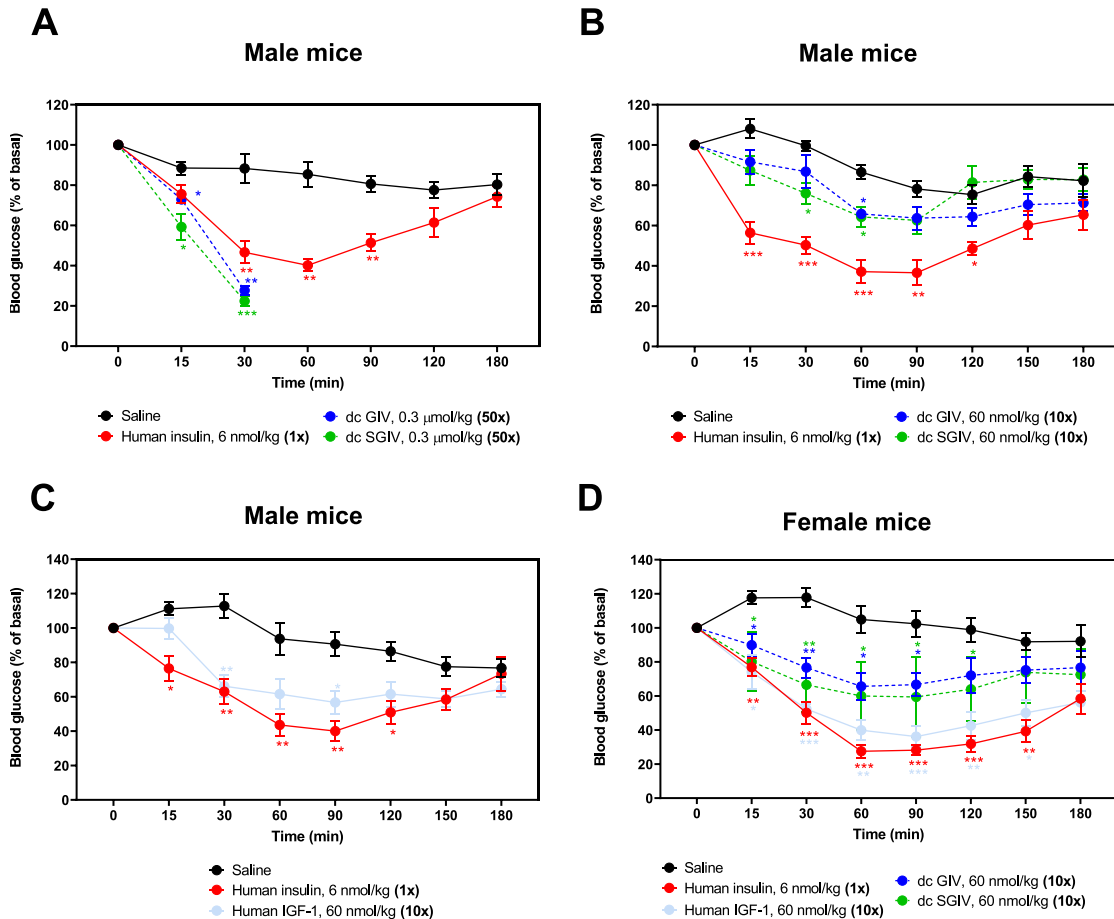
3.5. In vivo infusion experiments reveal WAT-specific effects of GIV dcVILP

To further explore the mechanism of dcVILP action in vivo, we performed an in vivo experiment using an acute administration of GIV dcVILP in awake mice. In this experiment, male C57BL/6J mice were intravenously infused with constant levels of tested ligand or insulin for 2 h, and 20% glucose was infused at variable rates to maintain

Table 2 — Receptor binding affinities of human insulin, human IGF-1, and dcVILPs to human IR-A, IR-B, and IGF1R receptors. Binding affinity is reported by the equilibrium dissociation constant (K_d). The K_d values were obtained from at least three independent measurements (indicated as n). Relative binding affinity is defined as K_d of human insulin or IGF-1/ K_d of ligand of interest.

Ligand	IR-A			IR-B			IGF1R		
	K_d [nM] \pm S.D. (n)	Relative to insulin (fold)	Relative to IGF-1 (fold)	K_d [nM] \pm S.D. (n)	Relative to insulin (fold)	Relative to IGF-1 (fold)	K_d [nM] \pm S.D. (n)	Relative to IGF-1 (fold)	Relative to insulin (fold)
Human insulin	0.52 \pm 0.03 (5)	1	202	0.58 \pm 0.07 (3)	1	303	293 \pm 101 (3)	0.0008	1
Human IGF-1	105 \pm 19 (4)	0.005	1	176 \pm 22 (3)	0.003	1	0.24 \pm 0.13 (3)	1	1221
dc GIV	315 \pm 81 (3)	0.002	0.33	1179 \pm 625 (3)	0.0005	0.15	41.3 \pm 11.6 (3)	0.006	7.09
dc SGIV	102 \pm 29 (3)	0.005	1.02	1441 \pm 558 (3)	0.0004	0.12	28.6 \pm 10.0 (3)	0.008	10.2
dc LCDV-1	no binding at 10^{-6} M (3)	—	—	$K_d > 10^{-5}$ M (3)	—	—	no binding at 10^{-6} M (3)	—	—

Insulin tolerance test



In vivo infusion experiments

Figure 3: GIV and SGIV dcVILPs stimulate glucose uptake in mice. A – D: Insulin tolerance test. C57BL/6J mice were injected i.p. with human insulin, human IGF-1, GIV, and SGIV dcVILPs or saline. The concentration of insulin was 6 nmol/kg in all panels, whereas the concentration of dcVILPs was 0.3 μmol/kg (A) and 60 nmol/kg (B, D). Concentration of human IGF-1 was 60 nmol/kg (C, D). Blood glucose was measured within the range from 0 to 180 min. Data are mean ± S.E.M. (*P < 0.05; **P < 0.01, ***P < 0.001). Mixed-effects analysis followed by Dunnett's multiple comparisons test was applied, n = 5 in all groups. **E:** Glucose infusion rates during the 2-hour in vivo experiments with infusion of human insulin or GIV dcVILP. The concentration of insulin was 0.015 nmol/kg/min, and the concentration of GIV dcVILP was 0.15 and 1.5 nmol/kg/min. n = 4 for insulin and n = 2 for both concentrations of GIV dcVILP. **F:** Glucose infusion rates during the 3-hour in vivo experiments with infusion of human insulin or GIV dcVILP. The concentration of insulin was 0.015 nmol/kg/min, and the concentration of dc GIV dcVILP was 0.75 nmol/kg/min. n = 4 for both groups. Two-way repeated measures ANOVA followed by Tukey's multiple comparisons test was applied. Data are mean ± S.E.M (*P < 0.05; **P < 0.01).

euglycemia. We first optimized the conditions using a 0.015 nmol/kg/min dose for insulin and 0.15 nmol/kg/min (10x) and 1.5 nmol/kg/min (100x) for GIV dcVILP. GIV dcVILP at 100x induced a strong glucose disposal as reflected by a profound increase in glucose infusion rate during the experiments, and there was a dose-dependent effect of GIV dcVILP as shown by a minimal effect of GIV dcVILP at 10x on glucose disposal in mice (Figure 3E). Based on this dose optimization experiment, we performed a 3-hour infusion of a 0.75 nmol/kg/min (50x) concentration of the GIV dcVILP and compared the effects to a 3-hour infusion of insulin at 0.015 nmol/kg/min in awake mice. Our data indicate that GIV dcVILP at 50x induced an increase in glucose disposal similar to insulin, as reflected by comparable rates of glucose infusion during the 3-hour experiments (Figure 3F).

In an additional cohort of mice, we performed a 3-hour infusion of 0.75 nmol/kg/min (50x) concentration of the GIV dcVILP or insulin at 0.015 nmol/kg/min with a continuous infusion of [$3\text{-}^3\text{H}$]glucose to assess whole body glucose turnover, and 2-deoxy-D-[$1\text{-}^{14}\text{C}$]glucose was administered as a bolus at 45 min before the end of experiments to measure glucose uptake in individual organs. Measurements of glucose uptake in heart, skeletal muscle (gastrocnemius), BAT (intrascapular) and WAT (epididymal) identified a unique characteristic of GIV dcVILP. While GIV dcVILP (50x) stimulated a comparable glucose uptake compared to insulin in gastrocnemius muscle, heart, and BAT (Figure 4A–C), the glucose uptake was significantly (1.9-fold) increased in WAT compared to insulin (Figure 4D). This finding suggests a tissue selective effect for GIV dcVILP on glucose metabolism in WAT.

Hepatic glucose production was significantly suppressed in both insulin and GIV dcVILP groups, but we did not determine any significant difference related to insulin action in the liver (Table S1). In separate experiments, we assessed insulin signaling in the liver, gastrocnemius muscle, and WAT and found that 50x GIV dcVILP stimulated phosphorylation of IR/IGF1R and Akt in all tissues (Figure 4E–G, Fig. S5). Akt phosphorylation was significantly increased by GIV dcVILP in the liver ($p = 0.0036$) (Fig. S5B). In WAT, Akt phosphorylation was significantly increased by GIV dcVILP ($p = 0.0238$), whereas this was not the case for insulin (Fig. S5F).

3.6. GIV dcVILP induces GLUT4 gene expression in WAT in vivo

To further understand the tissue selective effects of the GIV dcVILP observed for WAT, we used tissues collected at the end of a 3-hour in vivo infusion of GIV VILP or insulin in awake mice to evaluate the expression of the receptors and insulin-stimulated genes. Basal tissue samples were collected from mice after a 3-hour infusion of saline. Because our in vitro data showed that GIV dcVILP stimulates IGF1R more than insulin, we first explored the possibility that the GIV dcVILP-specific glucose uptake is caused by different receptor composition in different tissues. Using RT-qPCR, we showed that liver, BAT, and WAT contain the highest amounts of IR-B and low amounts of IR-A and IGF1R. In contrast, the most abundant receptor in skeletal muscle was IR-A (Fig. S6). These results showed that higher glucose uptake is not related to increased IGF1R expression in WAT. Next, we evaluated the expression of genes related to insulin action in liver, skeletal muscle (quadriceps), BAT, and WAT. Specifically, we focused on the genes related to glucose metabolism and lipogenesis. We also tested GLUT4 in all four tissues and thermogenesis marker uncoupling protein 1 (UCP-1) in BAT.

Consistent with our findings from in vivo glucose uptake, GLUT4 expression was significantly higher (1.5-fold) in GIV dcVILP-stimulated WAT compared to insulin-stimulated WAT (Figure 5A). Likewise, western blot analysis showed a trend of increase for GLUT4 protein in

GIV dcVILP-stimulated WAT compared to insulin-stimulated WAT insulin (Fig. S7). In addition to GLUT4, fatty acid synthase (FASN) expression was increased by 2.1-fold in GIV dcVILP compared to insulin (Figure 5B). Insulin and GIV dcVILP stimulated sterol regulatory element-binding protein 1-c (SREBP-1c) expression in a similar manner (Figure 5C), while GIV dcVILP showed an increasing trend for acetyl-CoA carboxylase 1 (ACACA) expression compared to insulin ($p = 0.087$, Figure 5D). We did not observe any significant differences between insulin and GIV dcVILP stimulated gene expression in any of the genes tested in muscle (Fig. S8) and BAT (Fig. S9).

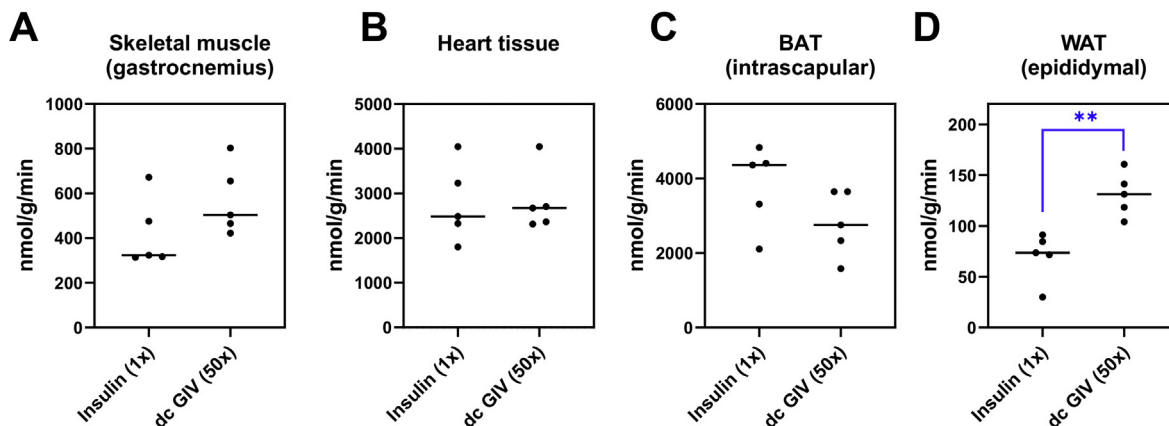
Consistent with previous studies on insulin action in the liver [47], the gluconeogenesis markers, catalytic subunit of glucose-6-phosphatase (G6PC) and phosphoenol pyruvate carboxykinase 1 (PCK1), were downregulated by both insulin and GIV dcVILP (Figure 6A,B), while glucokinase (GCK), the glycolysis marker, was upregulated (Figure 6C). We also observed a significant (1.6-fold) increase in GCK in the GIV dcVILP group compared to the insulin group. The lipogenesis markers were decreased by both insulin and GIV dcVILP (Figure 6D–G). Although the GLUT4 expression is very low in the liver [48], we observed a significant increase in GLUT4 expression after stimulation by GIV dcVILP when compared to both saline and insulin (4.7-fold) (Figure 6H). When we analyzed the receptor expression, both insulin and GIV dcVILP downregulated IR-B expression in the liver (Figure 6I), whereas only GIV dcVILP downregulated IGF1R expression (Figure 6J).

4. DISCUSSION

We recently discovered that four viruses belonging to the *Iridoviridae* family possess genes with high homology to human insulin and IGFs [9]. In this study, we characterized three of these VILPs in their insulin-like, i.e. double-chain, forms for the first time. We first showed that GIV and SGIV dcVILPs can bind to IR-A, IR-B, and IGF1R. Interestingly, on IR-A, the affinity of SGIV dcVILP is comparable to that of IGF-1, whereas the affinity of GIV dcVILP is 3x lower. On IR-B, however, the affinities of GIV and SGIV dcVILPs are comparable to each other and 7–8x lower than IGF-1. The only difference between IR-A and IR-B is 12 extra amino acids in the α -CT peptide that are present in IR-B but not IR-A [37,40]. This α -CT peptide is directly involved in ligand binding [28,29,31,32].

The sequences of GIV and SGIV dcVILPs differ only in three amino acids (Fig. S1), which correspond to insulin residues ValB2, ProB28, and SerA12. ValB2 and ProB28 have not been shown to be involved in the insulin:IR interaction, whereas SerA12 was shown to be involved in the Site 2 interaction [31,32]. SerA12 substitution by alanine decreases the affinity to IR to 36% of insulin [34]; however, SerA12 is known to be involved in interaction within IR FnIII-1 domain [31,32]. Therefore, SerA12 is unlikely to play a role in the differential binding to IR-A and IR-B. The only residue that lies in a region that is involved in interaction with the α -CT peptide (specifically C-terminal region of insulin B-chain [28,31,32]) is the residue corresponding to insulin ProB28. This residue is substituted by serine in GIV dcVILP, while proline is preserved in SGIV dcVILP. Therefore, it is probable that the ProB28Ser substitution lies behind the decreased affinity of GIV dcVILP to IR-A compared to SGIV dcVILP. By modeling of GIV and SGIV dcVILPs onto Site 1 of IR, we showed that the ProB28 presence makes the following ArgB28 and ArgB29 direct to the α -CT helix segment in SGIV dcVILP, while these residues are directed away from it in GIV dcVILP (Fig. S10A). Importantly, the last receptor amino acid in the model is Arg717 (PDB 6PVX), which is the last amino acid that is identical in IR-A and IR-B. After Arg717, there are three additional amino acids in IR-A, while there are 15 more amino acids in IR-B that

Tissue specific glucose uptake



In vivo insulin signaling

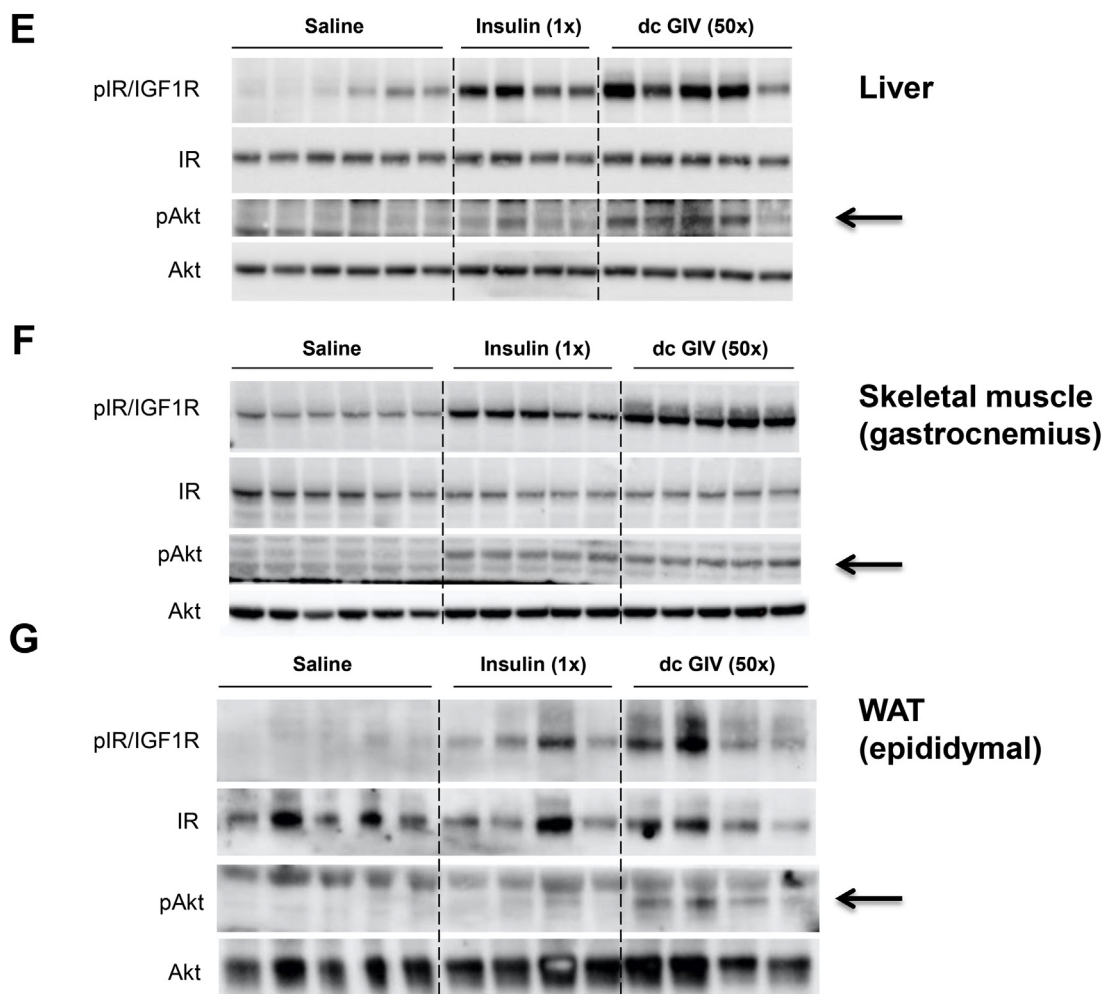


Figure 4: GIV dcVILP stimulates in vivo insulin signaling and WAT-specific glucose uptake. A–D: Tissue-specific glucose uptake after a 3-hour infusion of insulin (0.015 nmol/kg/min; 1x) or GIV dcVILP (0.75 nmol/kg/min; 50x) in awake mice (n = 5 for each group). Student's t-test was applied (**P < 0.01). n = 5 for both groups. E – G: in vivo signaling in insulin-sensitive tissues obtained at the end of 3-hour infusion of insulin (0.015 nmol/kg/min; 1x) or GIV dcVILP (0.75 nmol/kg/min; 50x) in awake mice. Basal tissue samples were collected after a 3-hour saline infusion. E: liver, F: skeletal muscle (gastrocnemius), G: WAT (epididymal). pAkt band is indicated by an arrow.

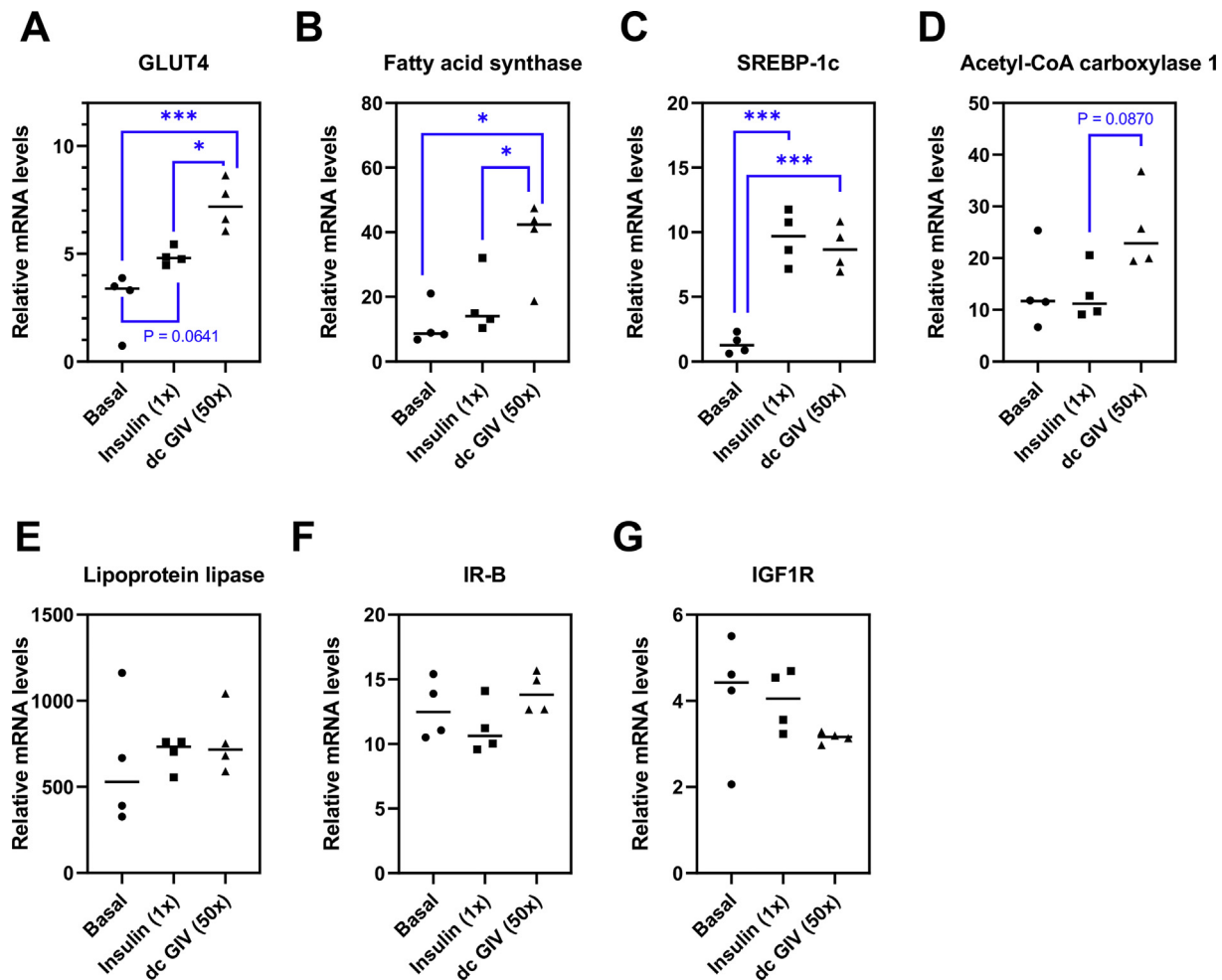


Figure 5: RT-qPCR analysis of expression of genes connected with insulin function and lipogenesis in murine WAT. Tissues were collected after 3-hour insulin (0.015 nmol/kg/min; 1x) or GIV VILP (0.75 nmol/kg/min; 50x) infusion, and basal tissue samples were collected after 3 h of saline infusion in awake mice. Data are expressed as % of β -actin. n = 4 per group. Ordinary one-way ANOVA followed by Tukey's multiple comparison test was applied (*P < 0.05; **P < 0.01, ***P < 0.001). P-values lower than 0.1 are indicated.

are not present in the model. Therefore, GIV dcVILP would potentially clash with the following α -CT sequence in both IR-A and IR-B, while SGIV dcVILP would avoid this clash in IR-A, but would still clash with the longer IR-B. This may explain why SGIV dcVILP has three-fold higher affinity for IR-A than GIV dcVILP, while their affinity for IR-B is comparable.

Another interesting observation is that GIV and SGIV dcVILPs have higher affinity to bind and stimulate signaling via IGF1R than insulin, since these ligands are missing the C-domain that is important for IGF-1:IGF1R interaction [49–52]. Even though dcVILPs are completely missing the C-domain, they bind to IGF1R with 7x (GIV dcVILP) and 10x (SGIV dcVILP) higher affinity compared to insulin. Signaling experiments are consistent with the binding results and showed a similar trend, as both GIV and SGIV dcVILPs stimulated phosphorylation of IGF1R, Akt, and Erk with higher potency than insulin. The comparison of amino acid sequences of GIV and SGIV dcVILPs with insulin and IGF-1 revealed that several amino acids that are involved in insulin binding to the Site 2 of IR are replaced in these VILPs by amino acids that are identical to IGF-1 in the corresponding positions and differ from insulin. Specifically, these include GluB10 (corresponding to Glu9 in IGF-1 and HisB10 in insulin), AspB13 (corresponding to Asp12 in IGF-1 and

GluB13 in insulin), and AspB21 (corresponding to Asp20 in IGF-1 and GluB21 in insulin) (Figure 1A). Interestingly, two of these three residues in IGF-1 (Glu9 and Asp12) are involved in IGF1R Site 1 binding. Comparisons of these two residues in models of GIV bound to the Site 2 of IR and Site 1 of IGF1R to human insulin (Fig. S10B) and IGF-1 (Fig. S10C) indicate that GIV and SGIV dcVILPs might preferentially bind to the Site 1 of IGF1R than to Site 2 of IR. This may be a possible explanation of why GIV and SGIV dcVILPs show an increased affinity and ability to activate IGF1R than insulin. Moreover, the HisB10Glu/Asp mutation in insulin is itself well known for dramatically enhancing the binding affinity to both IGF1R and IR-A [53–55].

One of the most interesting findings of this study is related to analysis of glucose uptake in the in vivo infusion experiments. Although the overall glucose infusion rates were slightly higher for 50x GIV dcVILP than insulin (1x), the differences between the ligands at these concentrations were not significant except for the two last time points (Figure 3F). Likewise, there were no significant differences in the tissue-specific glucose uptake in skeletal muscle, heart, and BAT. On the other hand, we showed that GIV dcVILP (50x) specifically stimulated 2-fold glucose uptake in epididymal WAT compared to insulin, which suggests specificity of GIV dcVILP action for WAT. To explore

whether this might be related with relatively higher amounts of IGF1R in WAT, we first explored the distribution of the receptors in insulin-sensitive tissues, but we did not observe an increased expression of IGF1R in WAT. Because we determined an increased Akt phosphorylation for GIV dcVILP compared to insulin in WAT, we decided to investigate the genes related to insulin action. We observed an increased GLUT4 and FASN expression in the GIV dcVILP group compared to insulin. This was specific to WAT and not observed in BAT and skeletal muscle. In the liver, glucokinase was significantly increased in mice receiving GIV dcVILP compared to insulin. The increase in glucokinase might be related with using an increased dose of GIV dcVILP compared to insulin.

Our results on GLUT4 expression are particularly interesting. Since its discovery in 1988 [56], there have been tremendous efforts to understand the function and regulation of GLUT4 [57]. Insulin is known to stimulate GLUT4 translocation [57,58] but not GLUT4 expression. Our data show that GIV dcVILP significantly stimulates GLUT4 expression in WAT. Further, both insulin and GIV dcVILP stimulated GLUT4 expression in BAT. These results indicate that GLUT4 expression in adipose tissue can be regulated by specific insulin analogs. Although we think that this is unlikely, we cannot completely exclude the possibility that the GLUT4 expression may be regulated by other pathways independent of PI3K/Akt and Ras/MAPK signaling. It was previously shown that GLUT4 expression is decreased in obesity and increased in response to exercise adipocytes [59]. Further, overexpression of GLUT4 in adipose tissue makes mice more insulin-sensitive and glucose tolerant [60,61]. Thus, identification and synthesis of novel insulin analogs targeting GLUT4 expression in adipose tissue might be a novel approach to be tested in diabetes control in the future.

To the best of our knowledge, GIV dcVILP is the first insulin analog that has WAT specificity, and further studies are needed to explain the specific mechanism underlying the tissue-selectivity. Previous studies have identified hepatoselective action for different insulin analogs [62–67]. This selectivity is thought to be related to either increased molecular size (proinsulin and insulin peglispro) or their ability to bind endogenous proteins (thyroxyl conjugates and insulin detemir) [68]. The increased data produced by genome projects have increased our ability to understand the natural repertoire of hormone ligands. For example, the Gila monster exendin-4 mimics GLP-1 functions, and unlike human GLP-1, it has a long half-life [69,70]. Likewise, recent discovery of cone snail venom insulins have potential to help us design fast-acting insulin analogs [71–73]. Thus, characterization of new VILPs that are evolved as a result of host–pathogen interactions and understanding the characteristics of tissue specificity has potential to help us design better insulin therapies.

While we did not identify any significant binding and signaling properties of LCDV-1 dcVILP on either of the receptors, its sc form was the most potent one of the three scVILPs in IGF-1R binding and in stimulating IR [9], suggesting an essential role of the C-peptide in these functions. On the other hand, the binding and signaling properties of GIV and SGIV scVILPs on IGF-1R were more comparable to insulin, which is more similar to the results obtained for their dc forms. Furthermore, while sc form of SGIV (1 $\mu\text{mol/kg}$, 166x) did not significantly lower the blood glucose in vivo, the dc form in both 60 nmol/kg (10x) and 0.3 $\mu\text{mol/kg}$ (50x) concentrations lowered the blood glucose confirming the important role of the double chain structure for the insulin-like function.

In our previous study, we showed that the sequences of these VILP-carrying viruses are identified in human fecal and plasma samples [9]. Although this finding suggests that humans are exposed to these

viruses, it remains unclear whether these fish viruses can infect humans. If they are found to infect humans, this will raise several questions regarding their link to human disease, including diabetes, cancer, and hypoglycemia. While the number of viruses that can infect mammalian animals are predicted to be over 320,000 [74], there are only 10,316 complete viral genomes in the NCBI database as of August 1, 2020. Thus, we expect to identify human viruses carrying VILPs in the future. Human viruses are known to target cellular metabolism by changing the expression levels of transcription factors, metabolic intermediates, and enzymatic activity [75–78]. We anticipate that VILP-carrying viruses are targeting the glucose metabolism and cell cycle when they infect fish to promote their replication. Furthermore, insulin and IGF-1 are mitogenic and anti-apoptotic molecules [79] that are two perfect characteristics that a pathogen needs. Indeed, overexpression of SGIV VILP stimulated cell proliferation in fish cells and increased SGIV replication [80].

5. CONCLUSIONS

Our study shows that GIV and SGIV dcVILPs are new members of the insulin/IGF superfamily with remarkable in vitro and in vivo insulin/IGF-1 like effects. Although we could not show binding competition for LCDV-1 dcVILP to human IR and IGF1R, it can stimulate a weak signal that requires further investigation. Identification of tissue selectivity of GIV dcVILP is novel and has potential to help us better understand the tissue selectivity of insulin. Furthermore, the effects of GIV dcVILP on GLUT4 expression opens a new avenue to better understanding of GLUT4 regulation by insulin action. In summary, our findings contribute to our understanding of VILP action on human receptors and have potential to help with designing new insulin/IGF analogs specific to WAT.

AUTHOR CONTRIBUTIONS

MC assisted with insulin tolerance test experiments, RNA extraction, qPCR analysis and insulin signaling experiments. FM and CRK assisted with in vivo signaling and insulin tolerance test. HLN, RHF and JKK conducted the in vivo infusion experiments in mice and obtained tissues for molecular analysis. JKK supervised the in vivo infusion experiments. LZ, JJ and TP assisted with binding competition experiments. FAV assisted with chemical synthesis of double-chain VILPs. EA, MC, JJ, CRK and JKK assisted with the analysis of the data. EA and MC wrote the manuscript, while all other authors contributed. EA designed the research and supervised the project.

ACKNOWLEDGEMENTS

This work was supported by the National Institute of Diabetes and Digestive and Kidney Diseases of the National Institutes of Health under award number K01DK117967 (to EA) and R01DK031026 and R01DK033201 (to CRK.). EA was also supported by The G. Harold & Leila Y. Mathers Foundation. The in vivo experiments in mice were conducted and tissues for molecular analysis were obtained from National Mouse Metabolic Phenotyping Center (MMPC) at UMass Medical School supported by an NIH grant (5U2C-DK093000 to JKK.). The research of TP, LZ, and JJ was supported by the Medical Research Council Grant MR/R009066/1 and by the Czech Academy of Sciences Project RVO 61388963. We would like to acknowledge Xiaochen Bai for the construction of the models of dcVILPs, Qian Huang for her help with qPCR protocol, and Boston College Biology Department undergraduate students Amaya Powis, Julianne Cutone, Kaan Sevgi and Maximilian Figura for their help with cell culture work.

CONFLICT OF INTEREST

None declared.

APPENDIX A. SUPPLEMENTARY DATA

Supplementary data to this article can be found online at <https://doi.org/10.1016/j.molmet.2020.101121>.

REFERENCES

- [1] De Meyts, P., 2004. Insulin and its receptor: structure, function and evolution. *BioEssays* 26:1351–1362.
- [2] Fernandez, R., Tabarini, D., Azpiazu, N., Frasc, M., Schlessinger, J., 1995. The *Drosophila* insulin receptor homolog: a gene essential for embryonic development encodes two receptor isoforms with different signaling potential. *The EMBO Journal* 14:3373–3384.
- [3] Nagasawa, H., Kataoka, H., Isogai, A., Tamura, S., Suzuki, A., Ishizaki, H., et al., 1984. Amino-terminal amino acid sequence of the silkworm prothoracicotropic hormone: homology with insulin. *Science* 226:1344–1345.
- [4] Pierce, S.B., Costa, M., Wisotzkey, R., Devadhar, S., Homburger, S.A., Buchman, A.R., et al., 2001. Regulation of DAF-2 receptor signaling by human insulin and *ins-1*, a member of the unusually large and diverse *C. elegans* insulin gene family. *Genes & Development* 15:672–686.
- [5] Chan, S.J., Steiner, D.F., 2000. Insulin through the ages: phylogeny of a growth promoting and metabolic regulatory hormone. *American Zoologist* 40:213–222.
- [6] Haeusler, R.A., McGraw, T.E., Accili, D., 2018. Biochemical and cellular properties of insulin receptor signalling. *Nature Reviews Molecular Cell Biology* 19:31–44.
- [7] Boucher, J., Kleinridders, A., Kahn, C.R., 2014. Insulin receptor signaling in normal and insulin-resistant states. *Cold Spring Harbor Perspectives in Biology* 6.
- [8] Smýkal, V., Pivarčí, M., Provazník, J., Bazalová, O., Jedlička, P., Lukšan, O., et al., 2020. Complex evolution of insect insulin receptors and homologous decoy receptors, and functional significance of their multiplicity. *Molecular Biology and Evolution* 37:1775–1789.
- [9] Altindis, E., Cai, W., Sakaguchi, M., Zhang, F., GuoXiao, W., Liu, F., et al., 2018. Viral insulin-like peptides activate human insulin and IGF-1 receptor signaling: a paradigm shift for host-microbe interactions. *Proceedings of the National Academy of Sciences of the United States of America* 115:2461–2466.
- [10] Huang, Q., Kahn, C.R., Altindis, E., 2019. Viral hormones: expanding dimensions in endocrinology. *Endocrinology* 160:2165–2179.
- [11] Tsai, C.T., Ting, J.W., Wu, M.H., Wu, M.F., Guo, I.C., Chang, C.Y., 2005. Complete genome sequence of the grouper iridovirus and comparison of genomic organization with those of other iridoviruses. *Journal of Virology* 79:2010–2023.
- [12] Song, W.J., Qin, Q.W., Qiu, J., Huang, C.H., Wang, F., Hew, C.L., 2004. Functional genomics analysis of Singapore grouper iridovirus: complete sequence determination and proteomic analysis. *Journal of Virology* 78:12576–12590.
- [13] Lopez-Bueno, A., Mavian, C., Labella, A.M., Castro, D., Borrego, J.J., Alcamí, A., et al., 2016. Concurrence of iridovirus, polyomavirus, and a unique member of a new group of fish papillomaviruses in lymphocystis disease-affected Gilthead sea bream. *Journal of Virology* 90:8768–8779.
- [14] Tidona, C.A., Darai, G., 1997. The complete DNA sequence of lymphocystis disease virus. *Virology* 230:207–216.
- [15] Fu, Z., Gilbert, E.R., Liu, D., 2013. Regulation of insulin synthesis and secretion and pancreatic Beta-cell dysfunction in diabetes. *Current Diabetes Reviews* 9:25–53.
- [16] Murphy, L.J., Bell, G.I., Friesen, H.G., 1987. Tissue distribution of insulin-like growth factor I and II messenger ribonucleic acid in the adult rat. *Endocrinology* 120:1279–1282.
- [17] McRory, J.E., Sherwood, N.M., 1997. Ancient divergence of insulin and insulin-like growth factor. *DNA and Cell Biology* 16:939–949.
- [18] Conlon, J.M., 2001. Evolution of the insulin molecule: insights into structure-activity and phylogenetic relationships. *Peptides* 22:1183–1193.
- [19] Smith, G.D., Pangborn, W.A., Blessing, R.H., 2003. The structure of T6 human insulin at 1.0 Å resolution. *Acta Crystallographica Section D Biological Crystallography* 59:474–482.
- [20] Vajdos, F.F., Ultsch, M., Schaffer, M.L., Deshayes, K.D., Liu, J., Skelton, N.J., et al., 2001. Crystal structure of human insulin-like growth factor-1: detergent binding inhibits binding protein interactions. *Biochemistry* 40:11022–11029.
- [21] Waterhouse, A., Bertoni, M., Bienert, S., Studer, G., Tauriello, G., Gumienny, R., et al., 2018. SWISS-MODEL: homology modelling of protein structures and complexes. *Nucleic Acids Research* 46:W296–W303.
- [22] Liu, F., Luo, E.Y., Flora, D.B., Mezo, A.R., 2014. A synthetic route to human insulin using isoacyl peptides. *Angewandte Chemie International Edition in English* 53:3983–3987.
- [23] Křížková, K., Chrudinová, M., Povalová, A., Selicharová, I., Collinsová, M., Vaněk, V., et al., 2016. Insulin-Insulin-like growth factors hybrids as molecular probes of hormone:receptor binding specificity. *Biochemistry* 55:2903–2913.
- [24] Morcavallo, A., Genua, M., Palummo, A., Kletvikova, E., Jiracek, J., Brzozowski, A.M., et al., 2012. Insulin and insulin-like growth factor II differentially regulate endocytic sorting and stability of insulin receptor isoform A. *Journal of Biological Chemistry* 287:11422–11436.
- [25] Kosinová, L., Veverka, V., Novotná, P., Collinsová, M., Urbanová, M., Moody, N.R., et al., 2014. Insight into the structural and biological relevance of the T/R transition of the N-terminus of the B-chain in human insulin. *Biochemistry* 53:3392–3402.
- [26] Cai, W., Sakaguchi, M., Kleinridders, A., Gonzalez-Del Pino, G., Dreyfuss, J.M., O'Neill, B.T., et al., 2017. Domain-dependent effects of insulin and IGF-1 receptors on signalling and gene expression. *Nature Communications* 8:14892.
- [27] Kim, J.K., 2009. Hyperinsulinemic-euglycemic clamp to assess insulin sensitivity in vivo. *Methods in Molecular Biology* 560:221–238.
- [28] Menting, J.G., Yang, Y., Chan, S.J., Phillips, N.B., Smith, B.J., Whittaker, J., et al., 2014. Protective hinge in insulin opens to enable its receptor engagement. *Proceedings of the National Academy of Sciences of the United States of America* 111:E3395–E3404.
- [29] Menting, J.G., Whittaker, J., Margetts, M.B., Whittaker, L.J., Kong, G.K., Smith, B.J., et al., 2013. How insulin engages its primary binding site on the insulin receptor. *Nature* 493:241–245.
- [30] Xu, Y., Kong, G.K., Menting, J.G., Margetts, M.B., Delaine, C.A., Jenkin, L.M., et al., 2018. How ligand binds to the type 1 insulin-like growth factor receptor. *Nature Communications* 9:821.
- [31] Uchikawa, E., Choi, E., Shang, G., Yu, H., Bai, X.C., 2019. Activation mechanism of the insulin receptor revealed by cryo-EM structure of the fully liganded receptor-ligand complex. *Elife* 8.
- [32] Gutmann, T., Schäfer, I.B., Poojari, C., Brankatschk, B., Vattulainen, I., Strauss, M., et al., 2020. Cryo-EM structure of the complete and ligand-saturated insulin receptor ectodomain. *The Journal of Cell Biology*, 219.
- [33] Li, J., Choi, E., Yu, H., Bai, X.C., 2019. Structural basis of the activation of type 1 insulin-like growth factor receptor. *Nature Communications* 10:4567.
- [34] De Meyts, P., 2015. Insulin/receptor binding: the last piece of the puzzle? What recent progress on the structure of the insulin/receptor complex tells us (or not) about negative cooperativity and activation. *BioEssays* 37:389–397.
- [35] Macháčková, K., Mlčochová, K., Potalitsyn, P., Hanková, K., Socha, O., Buděšínský, M., et al., 2019. Mutations at hypothetical binding site 2 in insulin and insulin-like growth factors 1 and 2 result in receptor- and hormone-specific responses. *Journal of Biological Chemistry* 294:17371–17382.

- [36] Gauguin, L., Delaine, C., Alvino, C.L., McNeil, K.A., Wallace, J.C., Forbes, B.E., et al., 2008. Alanine scanning of a putative receptor binding surface of insulin-like growth factor-I. *Journal of Biological Chemistry* 283:20821–20829.
- [37] Seino, S., Bell, G.I., 1989. Alternative splicing of human insulin receptor messenger RNA. *Biochemical and Biophysical Research Communications* 159: 312–316.
- [38] Peavy, D.E., Brunner, M.R., Duckworth, W.C., Hooker, C.S., Frank, B.H., 1985. Receptor binding and biological potency of several split forms (conversion intermediates) of human proinsulin. *Studies in cultured IM-9 lymphocytes and in vivo and in vitro in rats. Journal of Biological Chemistry* 260:13989–13994.
- [39] Sell, C., Dumenil, G., Deveaud, C., Miura, M., Coppola, D., DeAngelis, T., et al., 1994. Effect of a null mutation of the insulin-like growth factor I receptor gene on growth and transformation of mouse embryo fibroblasts. *Molecular and Cellular Biology* 14:3604–3612.
- [40] Frasca, F., Pandini, G., Scalia, P., Sciacca, L., Mineo, R., Costantino, A., et al., 1999. Insulin receptor isoform A, a newly recognized, high-affinity insulin-like growth factor II receptor in fetal and cancer cells. *Molecular and Cellular Biology* 19:3278–3288.
- [41] Miura, M., Surmacz, E., Burgaud, J.L., Baserga, R., 1995. Different effects on mitogenesis and transformation of a mutation at tyrosine 1251 of the insulin-like growth factor I receptor. *Journal of Biological Chemistry* 270:22639–22644.
- [42] Jiráček, J., Žáková, L., 2017. Structural perspectives of insulin receptor isoform-selective insulin analogs. *Frontiers in Endocrinology* 8.
- [43] Taniguchi, C.M., Emanuelli, B., Kahn, C.R., 2006. Critical nodes in signalling pathways: insights into insulin action. *Nature Reviews Molecular Cell Biology* 7:85–96.
- [44] Annunziata, M., Granata, R., Ghigo, E., 2011. The IGF system. *Acta Diabetologica* 48:1–9.
- [45] Nakano, K., Yanobu-Takanashi, R., Takahashi, Y., Sasaki, H., Shimizu, Y., Okamura, T., et al., 2019. Novel murine model of congenital diabetes: the insulin hyposecretion mouse. *Journal of Diabetes Investigation* 10:227–237.
- [46] Macotela, Y., Boucher, J., Tran, T.T., Kahn, C.R., 2009. Sex and depot differences in adipocyte insulin sensitivity and glucose metabolism. *Diabetes* 58:803–812.
- [47] Batista, T.M., Garcia-Martin, R., Cai, W., Konishi, M., O'Neill, B.T., Sakaguchi, M., et al., 2019. Multi-dimensional transcriptional remodeling by physiological insulin in vivo. *Cell Reports* 26:3429–34243 e3.
- [48] Karim, S., Adams, D.H., Lalor, P.F., 2012. Hepatic expression and cellular distribution of the glucose transporter family. *World Journal of Gastroenterology* 18:6771–6781.
- [49] Bayne, M.L., Applebaum, J., Underwood, D., Chicchi, G.G., Green, B.G., Hayes, N.S., et al., 1989. The C region of human insulin-like growth factor (IGF) I is required for high affinity binding to the type 1 IGF receptor. *Journal of Biological Chemistry* 264:11004–11008.
- [50] Gill, R., Wallach, B., Verma, C., Ursø, B., De Wolf, E., Grötzinger, J., et al., 1996. Engineering the C-region of human insulin-like growth factor-1: implications for receptor binding. *Protein Engineering* 9:1011–1019.
- [51] Bayne, M.L., Applebaum, J., Chicchi, G.G., Miller, R.E., Cascieri, M.A., 1990. The roles of tyrosines 24, 31, and 60 in the high affinity binding of insulin-like growth factor-I to the type 1 insulin-like growth factor receptor. *Journal of Biological Chemistry* 265:15648–15652.
- [52] Macháčková, K., Collinsová, M., Chrudinová, M., Selicharová, I., Pícha, J., Buděšínský, M., et al., 2017. Insulin-like growth factor 1 analogs clicked in the C domain: chemical synthesis and biological activities. *Journal of Medicinal Chemistry* 60:10105–10117.
- [53] Kurtzhals, P., Schaffer, L., Sorensen, A., Kristensen, C., Jonassen, I., Schmid, C., et al., 2000. Correlations of receptor binding and metabolic and mitogenic potencies of insulin analogs designed for clinical use. *Diabetes* 49: 999–1005.
- [54] Schwartz, G.P., Burke, G.T., Katsoyannis, P.G., 1987. A superactive insulin: [B10-aspartic acid]insulin(human). *Proceedings of the National Academy of Sciences of the United States of America* 84:6408–6411.
- [55] Slieker, L.J., Brooke, G.S., DiMarchi, R.D., Flora, D.B., Green, L.K., Hoffmann, J.A., et al., 1997. Modifications in the B10 and B26-30 regions of the B chain of human insulin alter affinity for the human IGF-I receptor more than for the insulin receptor. *Diabetologia* 40(Suppl 2):S54–S61.
- [56] James, D.E., Brown, R., Navarro, J., Pilch, P.F., 1988. Insulin-regulatable tissues express a unique insulin-sensitive glucose transport protein. *Nature* 333:183–185.
- [57] Klip, A., McGraw, T.E., James, D.E., 2019. Thirty sweet years of GLUT4. *Journal of Biological Chemistry* 294:11369–11381.
- [58] Brewer, P.D., Habtemichael, E.N., Romenskaia, I., Mastick, C.C., Coster, A.C., 2014. Insulin-regulated GLUT4 translocation: membrane protein trafficking with six distinctive steps. *Journal of Biological Chemistry* 289:17280–17298.
- [59] Huang, S., Czech, M.P., 2007. The GLUT4 glucose transporter. *Cell Metabolism* 5:237–252.
- [60] Tozzo, E., Shepherd, P.R., Gnudi, L., Kahn, B.B., 1995. Transgenic GLUT-4 overexpression in fat enhances glucose metabolism: preferential effect on fatty acid synthesis. *American Journal of Physiology* 268: E956–E964.
- [61] Shepherd, P.R., Gnudi, L., Tozzo, E., Yang, H., Leach, F., Kahn, B.B., 1993. Adipose cell hyperplasia and enhanced glucose disposal in transgenic mice overexpressing GLUT4 selectively in adipose tissue. *Journal of Biological Chemistry* 268:22243–22246.
- [62] Sinha, V.P., Choi, S.L., Soon, D.K., Mace, K.F., Yeo, K.P., Lim, S.T., et al., 2014. Single-dose pharmacokinetics and glucodynamics of the novel, long-acting basal insulin LY2605541 in healthy subjects. *The Journal of Clinical Pharmacology* 54:792–799.
- [63] Wang, Y., Shao, J., Zaro, J.L., Shen, W.C., 2014. Proinsulin-transferrin fusion protein as a novel long-acting insulin analog for the inhibition of hepatic glucose production. *Diabetes* 63:1779–1788.
- [64] Glauber, H.S., Revers, R.R., Henry, R., Schmeiser, L., Wallace, P., Kolterman, O.G., et al., 1986. In vivo deactivation of proinsulin action on glucose disposal and hepatic glucose production in normal man. *Diabetes* 35: 311–317.
- [65] Smeeton, F., Shojaae Moradie, F., Jones, R.H., Westergaard, L., Haahr, H., Umpleby, A.M., et al., 2009. Differential effects of insulin detemir and neutral protamine Hagedorn (NPH) insulin on hepatic glucose production and peripheral glucose uptake during hypoglycaemia in type 1 diabetes. *Diabetologia* 52:2317–2323.
- [66] Henry, R.R., Mudaliar, S., Ciaraldi, T.P., Armstrong, D.A., Burke, P., Pettus, J., et al., 2014. Basal insulin peglispro demonstrates preferential hepatic versus peripheral action relative to insulin glargine in healthy subjects. *Diabetes Care* 37:2609–2615.
- [67] Shojaae-Moradie, F., Powrie, J.K., Sundermann, E., Spring, M.W., Schuttler, A., Sonksen, P.H., et al., 2000. Novel hepatoselective insulin analog: studies with a covalently linked thyroxyl-insulin complex in humans. *Diabetes Care* 23:1124–1129.
- [68] Zaykov, A.N., Mayer, J.P., DiMarchi, R.D., 2016. Pursuit of a perfect insulin. *Nature Reviews Drug Discovery* 15:425–439.
- [69] Göke, R., Fehmann, H.C., Linn, T., Schmidt, H., Krause, M., Eng, J., et al., 1993. Exendin-4 is a high potency agonist and truncated exendin-(9-39)-amide an antagonist at the glucagon-like peptide 1-(7-36)-amide receptor of insulin-secreting beta-cells. *Journal of Biological Chemistry* 268:19650–19655.
- [70] Thorens, B., Porret, A., Bühler, L., Deng, S.P., Morel, P., Widmann, C., 1993. Cloning and functional expression of the human islet GLP-1 receptor.

- Demonstration that exendin-4 is an agonist and exendin-(9-39) an antagonist of the receptor. *Diabetes* 42:1678–1682.
- [71] Ahorukomeye, P., Disotuar, M.M., Gajewiak, J., Karanth, S., Watkins, M., Robinson, S.D., et al., 2019. Fish-hunting cone snail venoms are a rich source of minimized ligands of the vertebrate insulin receptor. *Elife* 8.
- [72] Robinson, S.D., Safavi-Hemami, H., 2016. Insulin as a weapon. *Toxicon* 123: 56–61.
- [73] Menting, J.G., Gajewiak, J., MacRaild, C.A., Chou, D.H., Disotuar, M.M., Smith, N.A., et al., 2016. A minimized human insulin-receptor-binding motif revealed in a *Conus geographus* venom insulin. *Nature Structural & Molecular Biology* 23:916–920.
- [74] Anthony, S.J., Epstein, J.H., Murray, K.A., Navarrete-Macias, I., Zambrana-Torrel, C.M., Solovyov, A., et al., 2013. A strategy to estimate unknown viral diversity in mammals. *mBio* 4:e00598–e00613.
- [75] Sanchez, E.L., Lagunoff, M., 2015. Viral activation of cellular metabolism. *Virology* 479–480:609–618.
- [76] Thai, M., Graham, N.A., Braas, D., Nehil, M., Komisopoulou, E., Kurdastani, S.K., et al., 2014. Adenovirus E4ORF1-induced MYC activation promotes host cell anabolic glucose metabolism and virus replication. *Cell Metabolism* 19:694–701.
- [77] Abrantes, J.L., Alves, C.M., Costa, J., Almeida, F.C., Sola-Penna, M., Fontes, C.F., et al., 2012. Herpes simplex type 1 activates glycolysis through engagement of the enzyme 6-phosphofructo-1-kinase (PFK-1). *Biochimica et Biophysica Acta* 1822:1198–1206.
- [78] Jordan, T.X., Randall, G., 2016. Flavivirus modulation of cellular metabolism. *Current Opinion of Virology* 19:7–10.
- [79] Kooijman, R., 2006. Regulation of apoptosis by insulin-like growth factor (IGF)-I. *Cytokine & Growth Factor Reviews* 17:305–323.
- [80] Yan, Y., Cui, H., Guo, C., Li, J., Huang, X., Wei, J., et al., 2013. An insulin-like growth factor homologue of Singapore grouper iridovirus modulates cell proliferation, apoptosis and enhances viral replication. *Journal of General Virology* 94:2759–2770.